

© 2008 IEEE. Personal use of this material is permitted. However, permission to reprint/republish this material for advertising or promotional purposes or for creating new collective works for resale or redistribution to servers or lists or to reuse any copyrighted component of this work in other works must be obtained from the IEEE.

This material is presented to ensure timely dissemination of scholarly and technical work. Copyright and all rights therein are retained by authors or by other copyright holders. All persons copying this information are expected to adhere to the terms and constraints invoked by each author's copyright. In most cases, these works may not be reposted without the explicit permission of the copyright holder.

# Encounter Modeling for Sense and Avoid Development

*Mykel J. Kochenderfer, Leo P. Espindle, J. Daniel Griffith, James K. Kuchar*  
*MIT Lincoln Laboratory, Lexington, Massachusetts*

## Abstract

Integrating unmanned aircraft into civil airspace requires the development and certification of systems for sensing and avoiding other aircraft. Because such systems are typically very complex and a high-level of safety must be maintained, rigorous analysis is required before they can be certified for operational use.

As part of the certification process, collision avoidance systems need to be evaluated across millions of randomly generated close encounters that are representative of actual operations. New encounter models are under development that capture changes that have occurred in U.S. airspace since earlier models were developed in the 1980s and 1990s. These models capture the characteristics of small, General Aviation aircraft that may not be receiving Air Traffic Control services as well as typically larger aircraft that are squawking a discrete transponder code. Both models allow dynamic changes in airspeed, vertical rates, and turn rates in a way that was not possible previously.

This paper describes the process used to construct the encounter models, how the models may be used in the development of sense-and-avoid systems for unmanned aircraft, and their application in an analysis of an electro-optical system for collision avoidance.

## Introduction

One of the main challenges to integrating unmanned aircraft into civil airspace is the development of systems that are able to sense and avoid local air traffic. If designed properly, these collision avoidance systems could provide an additional layer of protection that maintains or even enhances the current exceptional level of aviation safety. However, due to their safety-critical nature,

rigorous assessment is required before sufficient confidence can exist to certify collision avoidance systems for operational use. Evaluations typically include flight tests, operational impact studies, and simulation of millions of traffic encounters with the goal of exploring the robustness of the collision avoidance system. Key to these simulations are so-called encounter models that describe the statistical makeup of the encounters in a way that represents what actually occurs in the airspace.

One example system that has been rigorously tested in this manner is the Traffic alert and Collision Avoidance System (TCAS). As part of the TCAS certification process in the 1980s and 1990s, several organizations tested the system across millions of simulated close encounters and evaluated the risk of a near mid-air collision. This analysis ultimately led to the certification and U.S. mandate for TCAS equipage on larger transport aircraft. More recently, the International Civil Aviation Organization (ICAO) and Eurocontrol performed similar sets of simulation studies for European and worldwide TCAS mandates.<sup>1,2,3</sup>

The design of a collision avoidance system represents a careful balance to enhance safety while ensuring a low rate of unnecessary maneuvers. This balance is strongly affected by the types of encounter situations to which the system is exposed. It is therefore important that simulated encounters be representative of those that occur in the airspace. Hence, tremendous effort has been made by various institutions since the early 1980s to develop encounter models. The primary contribution of this paper is to introduce a new approach to encounter modeling that is based on a Bayesian statistical framework. The advantage of such a theoretical framework is that it allows us to optimally leverage available radar data to produce a model that is representative of the actual airspace.

---

This work is sponsored by the Air Force under Air Force Contract #FA8721-05-C-0002. Opinions, interpretations, conclusions, and recommendations are those of the authors and are not necessarily endorsed by the United States Government.

There are two factors leading to the need to update prior encounter models. Encounter models developed for TCAS involved only cooperative (transponder-equipped) aircraft typical of those that might be encountered by a transport aircraft and which are likely to be receiving air traffic control services. In addition, airspace has changed in the intervening 20 years due to new aircraft types (e.g., regional jets) and new procedures (e.g., the use of Reduced Vertical Separation Minimum at higher flight levels). Accordingly, our effort has been focused on both completely redesigning and updating the encounter model for cooperative aircraft to account for the current airspace and on developing an entirely new encounter model to represent aircraft not receiving air traffic control services.

While we use the same principled approach to develop the two models, the underlying assumptions behind each model are fundamentally different. The two models are termed “correlated” and “uncorrelated” respectively. We assume that the behavior of two aircraft in a correlated encounter are statistically related (i.e. what one aircraft is doing may be dependent on what the other aircraft is doing). Most correlations are assumed to be a function of Air Traffic Control (ATC) intervention and airspace structure. The uncorrelated model assumes that the air traffic environment is uniform; aircraft randomly encounter each other and neither aircraft affects what the other may be doing until they are close enough to use visual acquisition to maintain separation. While the correlated model is appropriate for aircraft receiving ATC services, the uncorrelated model represents situations involving aircraft flying under Visual Flight Rules (VFR) without flight following or without a transponder and which enter into a close encounter without any prior intervention taking place.

The next section describes the data that we use to construct the models. After explaining how to use our model to simulate new encounters, we demonstrate the utility of the model in a sensor-design trade study. We then summarize our conclusions and discuss further work.

## Radar Data

Our radar data stream comes from the 84th Radar Evaluation Squadron (RADES) at Hill AFB, Utah. RADES receives radar data from FAA and Department of Defense sites throughout the United States. They maintain continuous real-time feeds from a network of sensors, including long-range ARSR-4 radars around the perimeter of the United States and short-range ASR-8, ASR-9, and ASR-11 radars in the interior. Radar ranges vary from 60 to 250 NM. Figure 1 shows the coverage by the more than 120 sensors whose data was used to construct our model.

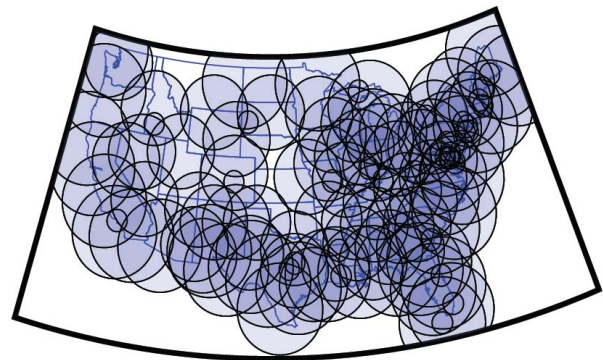


**Figure 1: Radar Coverage Map**

There are a number of advantages to our RADES data feed compared to the Enhanced Traffic Management System (ETMS) data often used in airspace analyses. ETMS data include only cooperative aircraft on filed Instrument Flight Rules flight plans and provides updates once per minute showing aircraft position after processing by air traffic control automation. In contrast, RADES data is continuously streaming directly from the radar, includes primary-only radar returns as well as all cooperative transponder returns (whether on a flight plan or not), providing track updates every 5 or 12 seconds without being affected by automation systems. This ensures that our filters and trackers have the best raw data with which to begin processing.

The National Offload Program (NOP) provides another potential data source. An advantage of NOP data is the inclusion of flight-plan and aircraft-type information. However, NOP data is post-automation, like ETMS, does not include data from

Department of Defense sensors, and does not have as comprehensive coverage as our RADES feed.

To build the uncorrelated model, we collected VFR (1200-code) beacon reports between December 1, 2007 and December 7, 2007, amounting to 30,000,000 reports representing 78,000 flight hours. The raw radar data is first processed using a tracking algorithm developed at Lincoln Laboratory.<sup>4</sup> A fusion algorithm, also developed at Lincoln Laboratory, then fuses tracks from multiple sensors to give one global view of all the tracks in U.S. airspace.<sup>5</sup> We eliminated tracks that had fewer than ten scans. We found that approximately ten scans are required to accurately estimate the various maneuver rates. We also eliminated tracks if any of their associated reports were inside Special Use Airspace whose boundaries are defined in the Digital Aeronautical Flight Information File (DAFIF), 8th Edition, managed by the National Geospatial-Intelligence Agency (NGA).

It is necessary to preprocess the raw radar data before features such as vertical rates and turn rates can be extracted to build our model. First, we remove outliers in the horizontal and vertical planes. In the horizontal plane, we remove jumps with ground speeds above 600 kt. In the vertical plane, we remove missing Mode C altitude reports and reports with vertical rates greater than 5000 ft/min or less than -5000 ft/min. After outlier removal, we discard tracks with fewer than ten valid scans. We then smooth the tracks using a Gaussian kernel to reduce the noise from the radar measurements. To get samples at 1 second intervals, we interpolate the smoothed reports using a piecewise-cubic Hermite interpolation scheme that preserves monotonicity and shape. The interpolated tracks are then ready for feature extraction and model building.

## Encounter Modeling

The primary function of an encounter model is the generation of random encounters that are representative of what occurs in the airspace. Given unlimited radar data, safety assessments could be performed using observed encounter events. However, because near mid-air collisions are so rare, it is necessary to generalize from the limited observed data to generate millions of test cases for a

robustness analysis. One of the primary challenges when constructing an encounter model is deciding how to best leverage the available radar data. The remainder of this section explains the variables defining the models, how we chose the relationships between them, and how we model dynamic variables.

### *Variables*

Another challenge is deciding which variables to use in the model. Certain variables, such as altitude layer and airspace class, are very important because they influence the characteristics of the encounter. For example, an aircraft at high altitude is more likely to be flying fast and straight, and aircraft in a terminal area is more likely to be turning and either climbing or descending.

For the uncorrelated model of VFR flight, we use the following variables:

- **Airspace class:** This variable may take on one of four values: B, C, D, and O, indicating which class of airspace the aircraft is in. The values B, C, and D correspond to the controlled airspace classes defined by the FAA. The value O represents “other airspace,” that is airspace, such as Class A, E, G, that is not B, C, or D. The airspace class variable was incorporated into our model to account for the variation in how aircraft fly in different airspace classes.
- **Altitude layer:** Airspace is also divided into four altitude layers. The first layer spans from 500 to 1200 ft Above Ground Level (AGL) to capture aircraft in the traffic pattern or performing low-level maneuvers. The second layer spans a transition zone from 1200 to 3000 ft AGL, the cruise altitude where the hemispheric rule begins. The third layer spans from 3000 ft AGL to 5000 ft AGL covering a mix of low-altitude enroute and maneuvering aircraft. The fourth layer includes airspace above 5000 ft AGL and would cover most enroute VFR traffic.
- **Airspeed:** We model true airspeed and allow it to vary during flight.

- **Acceleration:** Unlike previous encounter models, we allow airspeed acceleration to vary at every second.
- **Turn rate:** Turn rate is permitted to change every second in our model. The prior European and ICAO cooperative models allowed only a single turn during an encounter.
- **Vertical rate:** The vertical rate is permitted to change at every second. All prior cooperative models allowed only a single vertical acceleration period during an encounter.

The correlated encounter model has additional variables that capture the correlation between aircraft, including approach angle and horizontal and vertical miss distances at the time of closest approach.

### Markov Models

To model how the dynamic variables, such as turn rate and vertical rate, change over time we can use a Markov process. A Markov process is a stochastic process where the probability distribution over future states is determined only by the present state. In other words, one only needs to know the present state to predict the next state. Each state specifies a vertical rate, turn rate, and airspeed acceleration. Given an initial airspeed, horizontal coordinates, heading, vertical rate, altitude layer, and airspace class, we can infer from our model how the aircraft trajectory evolves over time.

### Dynamic Bayesian Networks

One of the challenges in using a Markov process to model is inferring the transition probabilities from limited data. Representing state transition probabilities explicitly requires specifying hundreds of millions of independent parameters (using a suitable level of variable discretization). Estimating the values of all of these parameters requires an infeasible amount of data. Fortunately, we can use dynamic Bayesian networks<sup>6</sup> to leverage the structure of the relationships between variables to greatly reduce the number of parameters.

A dynamic Bayesian network is a graphical structure consisting of nodes and directed edges. Figure 2 shows the dynamic Bayesian network used for the uncorrelated model. Dynamic Bayesian

networks have two slices. The first slice represents the values of variables at the current time step. The second slice represents the values of variables at the next time step. The arrows in the network represent direct statistical dependencies between variables.

For example, the vertical rate  $\dot{h}$  at time  $t + 1$  depends upon the vertical rate at time  $t$ , the airspace class  $A$ , and the altitude layer  $L$ . A conditional probability table associated with the node labeled  $\dot{h}(t + 1)$  specifies the probability distribution over vertical rates given the current vertical rate, airspace class, and altitude layer. For the dynamic Bayesian network in Figure 2, there are three conditional probability tables: one for vertical rate  $\dot{h}$ , one for turn rate  $\dot{\psi}$ , and one for airspeed acceleration  $\dot{v}$ . The number of parameters used to specify the Markov process is reduced from hundreds of millions to only thousands by using a dynamic Bayesian network. These parameter tables may be estimated from the radar data.

Once we decide upon a model structure and populate the conditional probability tables based on the radar data, we can sample from the network to produce new trajectories that are representative of the ones we observed in the radar data.

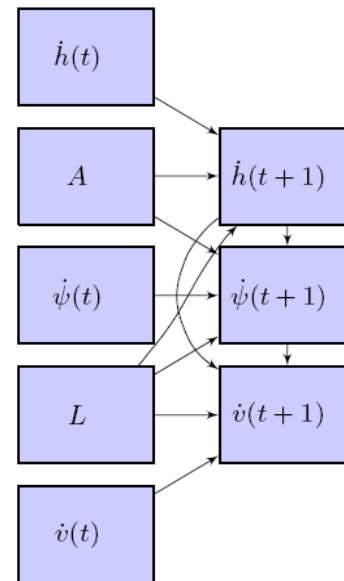


**Figure 2: Dynamic Bayesian Network Structure**

### ***Model Structure Identification***

Correctly identifying which relationships exist between variables in a dynamic Bayesian network is important. Not having directed edges between nodes when there is a true relationship between variables will result in an inaccurate model. Adding directed edges between nodes when relationships between variables are not truly present wastes data.

We use Bayesian statistical methods to determine how the variables are related to each other. Bayesian methods optimally balance model complexity with the amount of observed data. More data allows more relationships between variables to be captured in the model. This paper will not go into the details of how this is done, but details may be found in a paper by the authors elsewhere.<sup>7</sup> The Bayesian model selection approach involves searching for the graphical structure that maximizes its posterior probability given the data.

### **Simulation**

This section describes the initialization and simulation of an encounter between two aircraft.

An uncorrelated encounter occurs when an intruder penetrates an encounter cylinder centered on the own aircraft. The appropriate size for the encounter cylinder is determined by the aircraft dynamics and collision avoidance system. If the cylinder is too small, then the collision avoidance system does not have sufficient time to detect and track an intruder; however, if the cylinder is too large, then computation is wasted. In order to maintain the assumption that the density of aircraft traffic is uniform outside of the encounter cylinder, the process to initialize an uncorrelated encounter requires a random sampling and rejection approach. First, the intruder aircraft is randomly placed on the surface of the encounter cylinder about the own aircraft. The intruder aircraft is given an arbitrary heading. Next, the relative velocity vector between the two aircraft is calculated. If the relative velocity vector is such that the intruder aircraft is penetrating the encounter cylinder, then the encounter is kept. However, if this is not the case, then the aircraft is again randomly initialized on the surface of the encounter cylinder. This process continues until an acceptable initial condition is found. The resulting

distribution of intruder aircraft is demonstrated in Figure 3.

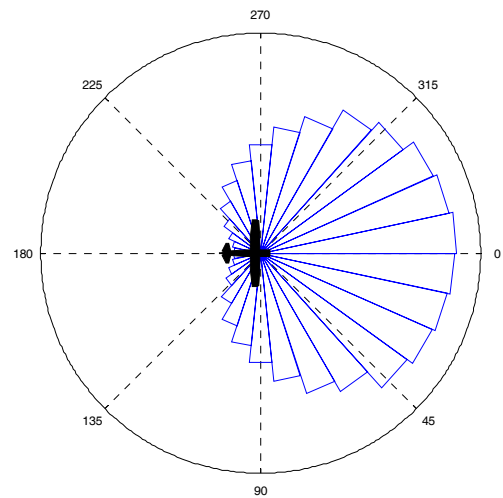


**Figure 3: Initial Intruder Bearing Distribution from Uncorrelated Model**

A different process is used to initialize a correlated (cooperative) encounter since vertical miss distance, horizontal miss distance, and approach angle are defined by the encounter model. First, both aircraft are run through the simulation open-loop (i.e. without TCAS or any other collision avoidance system enabled). Second, the aircraft initial positions and headings are rotated and translated so that the vertical miss distance, horizontal miss distance, and approach angle defined by the encounter model all occur at the time of closest approach.

In order to simulate the encounters we use Lincoln Laboratory's Collision Avoidance System Safety Assessment Tool (CASSATT), which performs fast-time Monte Carlo analysis that takes encounter model data as an input and simulates aircraft motion while the intruder aircraft is inside the encounter cylinder for uncorrelated encounters or a predetermined length of time for correlated encounters. The simulation has several integrated sub-models including TCAS, sense-and-avoid sensor models and algorithm logic, 3D airframe models, a human visual acquisition model, a pilot response model, command and control latency, and an adjustable vehicle dynamics model. Aircraft motion is represented using 6 degree-of-freedom or 4 degree-of-freedom point-mass dynamics with

acceleration constraints and transient response characteristics related to aircraft type.

We simulate the encounters using Lincoln Laboratory's parallel computing environment.<sup>8</sup> A large Monte Carlo run on the order of a million encounters can be simulated in a few hours and is generally sufficient to evaluate the overall safety of a collision avoidance system. Typical metrics for evaluating a collision avoidance system include miss distances, risk ratios, and near mid-air collision rate.

## Sense and Avoid Analysis

The Department of Defense and Department of Homeland Security are particularly interested in applying an uncorrelated model to the analysis of unmanned aircraft sense and avoid capabilities. To date, there has not been a rigorous analysis of collision avoidance systems on unmanned aircraft in encounters with air traffic without transponders.

Sense and avoid capabilities on unmanned aircraft are currently not mature enough to meet the FAA requirement for integrating unmanned aircraft into civil airspace. Although collision avoidance systems are under development for unmanned aircraft, no system has been certified for routine use by the FAA.

In order to meet the FAA safety requirements, developers of unmanned systems are considering a variety of onboard sensors. These include the Traffic alert and Collision Avoidance System (TCAS), automatic dependent surveillance-broadcast (ADS-B), electro-optical (EO) and infrared (IR) systems, radar, and acoustic systems. TCAS and ADS-B provide a satisfactory means of sensing appropriately-equipped aircraft but lack the ability to detect aircraft that are not equipped with the proper avionics. EO, IR and radar sensors are attractive solutions for detecting traffic because they do not require that intruders have special equipment. EO and IR systems are particularly attractive for unmanned aircraft since their power requirements and payload sizes are smaller than radar systems.

A white paper issued by Air Combat Command defines sense and avoid requirements for unmanned aircraft that require access to civil airspace without a Federal Aviation Administration

(FAA) Certificate of Authorization (COA).<sup>9</sup> The purpose of the white paper is to provide an initial, formal sense and avoid requirement for unmanned aircraft to ensure that unmanned aircraft comply with all applicable regulations for operating in all classes of airspace.<sup>10</sup> The white paper sense and avoid requirements for Field of View (FOV) are based on both NASA and Department of Defense studies, as well as the Convention on International Civil Aviation, Annex 2, Rules of the Air, and stipulate  $\pm 110^\circ$  in azimuth and  $\pm 15^\circ$  in elevation.<sup>11</sup> The current electro-optical system that has been test flown for potential use on Global Hawk has a slightly smaller azimuth angle ( $\pm 100^\circ$ ) due to cost constraints.

This section presents a parametric analysis of the sense and avoid capability of an electro-optical system for unmanned aircraft. We assess the exchange between the sensor FOV azimuth and elevation angles with the probability of intruder detection prior to near miss for encounters that result in a Near Mid-Air Collision (NMAC, which we define as a loss in separation of 500 ft horizontally and 100 ft vertically at the same time). More extensive analysis that includes an assessment of the effect of varying detection range and the trade-offs between FOV azimuth angle and probability of detection with fixed tracking technology (i.e. pixel array sensor and tracking algorithm) can be found in Griffith et al.<sup>12</sup>

In addition, Kochenderfer et al.<sup>13</sup> analyze an EO hazard alerting system based on intruder line-of-sight rate measurements from simulations of uncorrelated encounters.

## Encounter Characteristics

We use two collections of 1 million encounters each as the basis for our analysis. One collection consists of encounters between pairs of VFR aircraft generated by the uncorrelated encounter model. The other collection consists of encounters between a notional Global Hawk and VFR aircraft. The Global Hawk trajectories are a mixture of four representative profiles, as shown in Table 1. The first two profiles were extracted from radar data of an actual Global Hawk flight from Beale AFB, CA. The other two profiles were based on Global Hawk performance specifications. The first two profiles in the table have average climb rate, turn rate, and

airspeed listed since they vary during the course of the trajectory. All other values in the table are constant.

**Table 1: Representative Global Hawk Profiles**

Proportion	Climb rate (ft/min)	Turn rate (deg/s)	True Airspeed (kt)
25%	3392	1.5	191
25%	-1279	0.2	145
25%	3100	0	170
25%	-1300	0	150

Table 2 summarizes the characteristics of the two encounter sets. We used a larger encounter cylinder height for encounters involving Global Hawk because the airspeed and vertical rates of Global Hawk are greater than typical VFR aircraft. Of particular note is that the minimum simulation time to minimum cylindrical distance (TMCD)<sup>2</sup> for the encounter sets is greater than 25 s, which is sufficient time for a collision avoidance system to sense and avoid an intruder. Also of note, the distribution of intruders is more concentrated towards zero bearing for Global Hawk than VFR aircraft because the airspeed of Global Hawk is higher than most VFR aircraft in our model. Thus, intruders are less likely to overtake Global Hawk. As shown in Table 2, a fraction of the million intruders that were tested resulted in an actual Near Mid-Air Collision (NMAC) event; these are termed NMAC intruders.

***Electro-Optical Configuration Trade-offs***

Results are presented here in terms of detection probability. Detection probability in this analysis depends only on whether the intruder is within both the FOV and range limits specified, assuming an ideal sensor. This metric does not take into account the behavior of the detector array, the apparent size of the intruder, or processing/tracking algorithms. Thus, it is likely that the actual detection probability

<sup>2</sup> Cylindrical distance is  $\max(r_h/5, r_v)$ , where  $r_h$  is horizontal range and  $r_v$  is vertical range.

would be somewhat lower than estimated here due to sensor and processing inefficiencies.

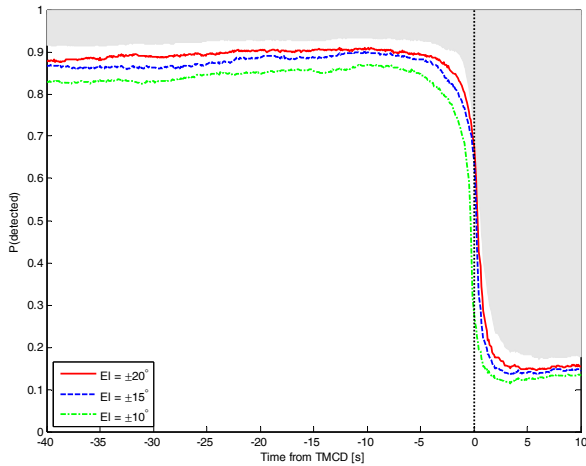
**Table 2: Characteristics of the Two Collections of 1 Million Encounters**

	VFR/VFR	Global Hawk/VFR
Encounter cylinder radius	5 NM	5 NM
Encounter cylinder height	±1500 ft	±3300 ft
Minimum TMCD (simulation time)	27.9 s	30.4 s
Mean TMCD (simulation time)	166.4 s	89.4 s
NMACs (per million encounters)	541	364

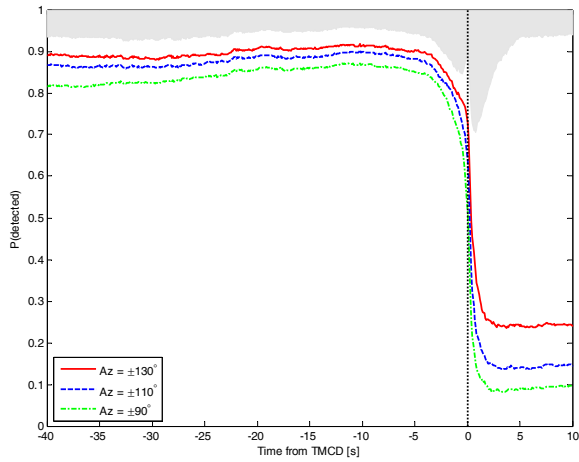
Figure 4 presents the detection probability of an NMAC intruder during the 40 second window prior to TMCD for VFR/VFR encounters with various elevation angles for a fixed azimuth angle of  $\pm 110^\circ$  and detection range of 5 NM. The various lines in the plot represent different elevation FOV conditions. As shown, approximately 80%-90% of the NMAC intruders are within the range and FOV constraints until 10 s before closest approach. Near the time of closest approach, the relative motion of intruders increases rapidly and they typically leave the FOV. The shaded gray region corresponds to infeasible values when varying the single configuration parameter. For example, the detection probability cannot be raised above 90% regardless of elevation FOV because the azimuth FOV angle is fixed at  $\pm 110^\circ$ .

Figure 5 plots detection probability with respect to azimuth angles when the FOV elevation angle is  $\pm 15^\circ$  with a 5 NM detection range. Figure 4 and Figure 5 together indicate that the sensitivity of probability of detection with respect to the FOV angles is locally small for the current design configuration. Slightly increasing or decreasing the azimuth and elevation angles has minimal impact on the detection probability of an NMAC intruder prior to near miss. For example, increasing the

azimuth angle from  $\pm 90^\circ$  to  $\pm 130^\circ$  only results in approximately a 10% increase in the probability of detection at any point prior to near miss.



**Figure 4: Effect of Varying Elevation Angle (VFR/VFR)**



**Figure 5: Effect of Varying Azimuth (VFR/VFR)**

The results from the Global Hawk/VFR encounters lead to slightly different conclusions. Figure 6 shows the effect of varying elevation angle when the FOV azimuth angle is  $\pm 110^\circ$  and the detection range is 5 NM. The FOV elevation angle on Global Hawk has a greater influence on probability of detection than in the VFR/VFR encounter case. The increased sensitivity to elevation angle is a byproduct of the steep Global

Hawk climb profile. Since Global Hawk may be both climbing and turning, its FOV may be rotated out of the horizontal plane and not be pointed in the direction of the future path of the vehicle. A significant portion of NMAC intruders are above or below the FOV. One option to improve the probability of detection for the EO sensor is to increase the elevation angle over the entire FOV. However, there are other feasible options. Another choice is to reduce the frequency that Global Hawk turns as it climbs or descends through airspaces where encounters are likely to occur. This ensures that the FOV is pointed in the direction of the future path of the Global Hawk vehicle. A second choice is to modify the EO sensor such that the FOV is bow-tie shaped. In a bow-tie shaped FOV concept, the middle, forward-facing camera has a small FOV with a high resolution while the outer cameras provide wide area coverage that capture intruders during turning maneuvers. A further option is to horizontally stabilize the EO sensor. By counteracting the effect of the unmanned aircraft's bank angle, other analysis has shown that nearly all of the intruders are in view within the 40 second window prior to near miss. In particular, there are on average 23% more intruders within the FOV per time-step when the EO sensor is horizontally stabilized in the Global Hawk climb out profile.

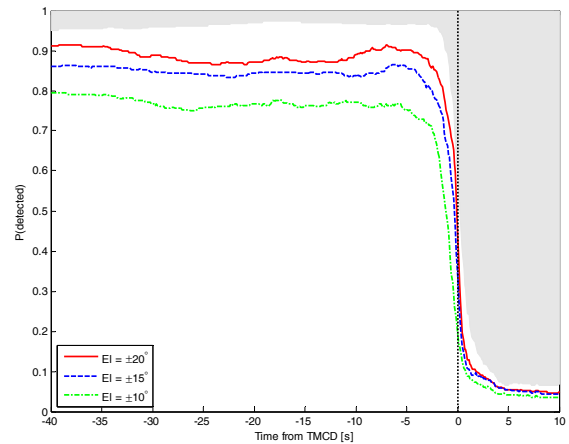


**Figure 6: Effect of Varying Elevation Angle (Global Hawk/VFR)**

Figure 7 presents the effect of azimuth when the elevation angle is fixed at  $\pm 15^\circ$ . Detection probability is locally insensitive to changes in the FOV azimuth angle. The current, flight-tested

sensor configuration with a  $\pm 100^\circ$  azimuth angle is just as likely to detect an intruder prior to near miss as an EO sensor that meets the standard configuration with a  $\pm 110^\circ$  azimuth angle. In fact, the azimuth angle can be further reduced to  $\pm 90^\circ$  without degrading detection probability. Since Global Hawk's airspeed is higher than that of most intruders, there is a smaller probability that a VFR intruder will cause an NMAC from a large bearing angle (e.g., an overtaking encounter). Encounters that result in an NMAC with Global Hawk are more concentrated towards zero bearing in our simulation. Note however that the results would likely be different when using the correlated encounter model since that model contains faster-flying aircraft.

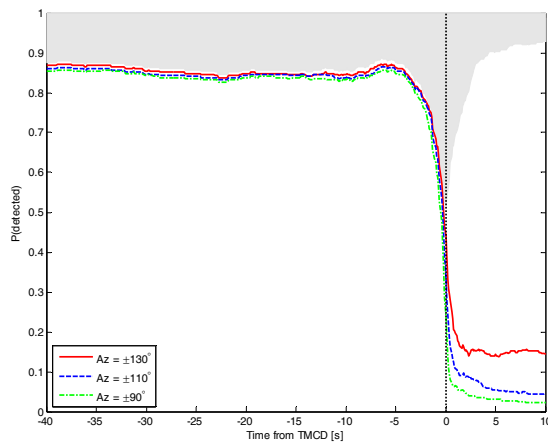


**Figure 7: Effect of Varying Azimuth (Global Hawk/VFR)**

Previous studies claim that a slightly reduced FOV ( $\pm 100^\circ$  azimuth angle) is desirable for testing purposes since it is significantly less expensive to develop.<sup>14</sup> Our analysis suggests that upgrading the FOV azimuth angle to  $\pm 110^\circ$  does not appreciably increase system performance due to the airspeed of Global Hawk in our simulation. Instead, better performance may be realized by improving detection range or increasing the elevation angle. While the current estimated detection range is suitable for nominal conditions, several factors such as weather and intruder aircraft size can reduce the effective detection range of the EO sensor. Additional testing using the correlated encounter model is also necessary to examine performance against a wider range of aircraft types.

These observations suggest that the FOV for an EO system that maximizes probability of detecting intruders and, thus, the level of safety of the unmanned aircraft is a function of the aircraft's airspeed and flight profile. A slow flying unmanned aircraft requires a wider FOV than a faster aircraft since overtaking encounters are more likely. In contrast, the faster vehicle requires a larger detection range since the closure rates of intruder aircraft are generally higher.

## Summary and Further Work

This paper has presented a new approach to modeling close encounters in the national airspace. The correlated and uncorrelated encounter models will play an important role in the development and certification of sense-and-avoid systems for unmanned aircraft. A full report on uncorrelated encounter modeling is available from the authors. In addition, a complete report on the correlated encounter model will be available September 2008.

The last part of this paper demonstrates the types of analysis the models can support. Using the uncorrelated model, we assessed the exchange between the sensor field-of-view azimuth and elevation angles with the probability of intruder detection prior to near miss. Future studies will examine the safety of end-to-end systems, including both sensor performance and the effects of avoidance maneuvers.

## Acknowledgments

We wish to acknowledge the support provided by Maj. Luke Cropsey, Lt. Col. Kent Tiffany, and Mr. Tony Salmonson of 303 AESW/XXR at Wright-Patterson Air Force Base.

## Email Addresses

[mykelk@ll.mit.edu](mailto:mykelk@ll.mit.edu), [espindle@ll.mit.edu](mailto:espindle@ll.mit.edu),  
[dan.griffith@ll.mit.edu](mailto:dan.griffith@ll.mit.edu), [kuchar@ll.mit.edu](mailto:kuchar@ll.mit.edu)

## References

<sup>1</sup> ICAO, 1998, Surveillance, radar and collision avoidance. ICAO Standards and Recommended Practices, volume IV, annex 10.

---

<sup>2</sup> Thierry Miquel and Kevin Rigotti, 2002, European encounter model. Technical Report ACASA/WP1/186/D, CENA/Sofréavia and QinetiQ.

<sup>3</sup> Stéphan Chabert, 2005, Safety encounter model focused on issue SA01a. Technical Report SIRE/WP2/21/D, CENA/Sofréavia and QinetiQ.

<sup>4</sup> Robert D. Grappel, 2001, ASR-9 processor augmentation card (9-PAC) phase II scan-scan correlator algorithms. Technical Report MIT-LIN-ATC-298, MIT Lincoln Laboratory.

<sup>5</sup> Jeffrey L. Gertz, 1983, Mode S surveillance netting. Technical Report MIT-LIN-ATC-120, MIT Lincoln Laboratory.

<sup>6</sup> Kevin Murphy, 2002, Dynamic Bayesian Networks: Representation, Inference and Learning, PhD thesis, University of California, Berkeley.

<sup>7</sup> Mykel J. Kochenderfer, Leo P. Espindle, James K. Kuchar, J. Daniel Griffith, 2008, A Bayesian Approach to Aircraft Encounter Modeling, submitted for publication to AIAA Guidance, Navigation, and Control Conference and Exhibit, Honolulu, HI.

<sup>8</sup> N.T. Bliss, R. Bond, J. Kepner, H. Kim, and A. Reuther, 2006, Interactive Grid Computing at Lincoln Laboratory, Lincoln Laboratory Journal, Vol. 16, No. 1, pp. 165-216, Lexington, MA.

<sup>9</sup> M. D. Ebdon, and J. Regan, 2004, Sense-and-Avoid Requirement for Remotely Operated Aircraft (ROA), Air Combat Command, Langley Air Force Base, VA.

<sup>10</sup> Federal Aviation Administration, February 2004, Order 7610.4K: Special Military Operations. Washington, D.C.

<sup>11</sup> ICAO, July 1990, Rules of the Air, Annex 2 to the Convention on International Civil Aviation, Chicago, IL.

<sup>12</sup> J. Daniel Griffith, Mykel J. Kochenderfer, and James K. Kuchar, 2008, Electro-Optical System Analysis for Sense and Avoid, submitted for publication to AIAA Guidance, Navigation, and Control Conference and Exhibit, Honolulu, HI.

<sup>13</sup> Mykel J. Kochenderfer, J. Daniel Griffith, and James K. Kuchar, 2008, Hazard Alerting using

---

Line-of-Sight rate, submitted for publication to AIAA Guidance, Navigation, and Control Conference and Exhibit, Honolulu, HI.

<sup>14</sup> John McCalmont, James Utt, Mike Deschenes, and Michael Taylor, 2005, Sense and Avoid, Phase I (Man-in-the-Loop) Advanced Technology Demonstration, Infotech@Aerospace, Arlington, VA.

*2008 ICNS Conference*

*5-7 May 2008*